JOURNAL OF SPACECRAFT AND ROCKETS
Vol. 34, No. 3, May–June 1997

Thermal Sensitivity Analysis of Spacecraft Battery

S. Suresha*
Indian Space Research Organisation Satellite Centre, Bangalore 560 017, India
S. C. Gupta†
Indian Institute of Science, Bangalore 560 012, India
and
R. A. Katti‡
Indian Space Research Organisation Satellite Centre, Bangalore 560 017, India

Transient thermal sensitivity is studied for systems that are subjected to conductive heat transfer within themselves and radiative heat transfer with the surrounding environment, including solar heat radiation. The battery in the Indian national communication satellite is one such system for which the studies are conducted with respect to panel conduction, conductance of insulating blanket, power dissipation within the battery, and absorptance and emittance of various elements. Comparison of sensitivities revealed that battery temperature is sensitive to its power dissipation during the beginning of life of the spacecraft, whereas toward the end of life of the spacecraft mission, the effect of absorptance of optical solar reflector is dominating. The influence of optical property values of the multilayer insulation blanket is almost negligible. Among the parameters studied in this analysis, the battery temperature is found to be most sensitive to emittance of the optical solar reflector.

Nomenclature

A	= total surface area of the nodal element exposed to solar radiation, m^2
A_c	= cross-sectional area of the nodal element, m^2
A_s	= surface area of the nodal element, m^2
c_p	= heat capacity at constant pressure, J/kg K
$F_{i,j}$	= geometrical view factor between the ith and the jth elements or nodes
g_i	= heat generated at the ith node, W
k_{x_i}	= thermal conductivity of the material in the x_i direction, where i is 1, 2, 3, W/m K
$l_{i,j}$	= linear elemental length between ith and jth node, m
m_i	= mass of the ith nodal element, kg
N	= total number of nodes or elements in the system
S_i^n	= sensitivity function for the ith node at the nth time step, K/unit of the parameter considered
S_{ri}	= semirelative sensitivity function for the ith node, K
s	= solar intensity, W/m^2
T_i	= temperature of the ith element or node, K
t	= time, s
(x_1, x_2, x_3)	= Cartesian coordinate of a system, m
α	= solar absorptance of surface
Δt	= time step in numerical integration, s
Δx_1	= differential length along x_1 direction, m
ε	= infrared emittance of the surface
θ	= angle between the surface normal and the sun vector
ρ	= density of the material, kg/m^3
σ	= Stefan–Boltzmann constant, W/m^2 K^4

Subscripts

i, j	= ith and jth node
l, m	= lth and mth element
S_p	= space

Superscripts

n	= nth time step
r	= rth iteration

Received June 14, 1996; revision received Oct. 22, 1996; accepted for publication Nov. 10, 1996.

*Scientist, Thermal Systems Group.
†Professor, Department of Mathematics.
‡Head, Thermal Analysis Section.

Introduction

THERMAL design for a system with a narrow allowable temperature range requires an in-depth thermal analysis of the system with respect to its design parameters. Design parameters comprise thermophysical and optical properties of the thermal control elements, interface conductance, internal heat dissipation, external heat flux, etc. Knowledge of the dependence of the system temperature on these parameters helps in devising an optimal thermal design for a system.

Studies in thermal sensitivities have been conducted by several researchers. Goble[1] discussed the steady-state sensitivities to estimate temperature uncertainties that arise due to uncertainties in the physical parameters associated with the mission of the Skylab orbital assembly. Transient thermal sensitivity analysis was conducted by Haftka[2] on the insulation for the aluminum structure proposed for the space transportation system. Haftka and Malkus[3] did a similar analysis for the insulated aluminum cylinder proposed for a similar system. In these studies, steady-state, as well as transient, sensitivity functions have been evaluated under the system-imposed constraints. The efficiency of the technique depends on the ratio of number of constraints to the number of design parameters. Tortorelli et al.[4] formulated the design sensitivities for nonlinear transient systems using a Lagrange multiplier and convolution theory. Lomos and Eppel[5] did a sensitivity analysis for solar buildings. Guru Prasad and Kane[6] conducted a thermal shape sensitivity analysis using the boundary element method. Wiedemann[7] showed the utility of simulation and sensitivity analysis in determining thermal parameters associated with the microsystems. Two methods, direct differentiation and the adjoint variable method, were discussed by House et al.[8] to study the design sensitivities of a thermal system. Thermal modeling and its application to advanced battery systems were studied by Johnsee.[9] In the present study, transient thermal sensitivities have been evaluated for the Ni-Cd battery used in Indian National Satellite System. The mathematical model is reduced to a system of nonlinear coupled first-order differential equations. Numerical methods employed to solve the nonlinear coupled differential equations are discussed and numerical results are presented. The quasisteady-state temperatures and sensitivity functions at the beginning of life (BOL) and at the end of life (EOL) of the spacecraft mission are

computed and analyzed. Computations are done for the nominal parameter values[10] at the BOL and at the EOL.

Problem Formulation

A system in a space environment, whether mechanical, electrical, or electronic, can be assumed to be made up of number of solid elements. There exists conductive heat transfer within connected solid elements. The external surfaces of any solid element participates in radiative heat transfer with the surfaces of the other solid elements, including space. The external surfaces are exposed to incident solar heat fluxes, which are time dependent. The Earth shine load and albedo load are considered to be negligible as the orbit is geostationary. Considering the internal heat generation for an element, the Fourier heat conduction equation for an mth element in a system can be written as

$$\rho_m c_{p_m} \frac{\partial T_m}{\partial t} = \left[k_{x_1} \frac{\partial^2 T_m}{\partial x_1^2} + k_{x_2} \frac{\partial^2 T_m}{\partial x_2^2} + k_{x_3} \frac{\partial^2 T_m}{\partial x_3^2} + g_m \right] \tag{1}$$

The boundary conditions on the surfaces of this element are defined as

$$-k_{x_i} \frac{\partial T_m}{\partial_{x_i}} = \left[\sum_{l=1}^{N} \sigma \varepsilon_m F_{m,l} A_{s_m} \left(T_m^4 - T_l^4 \right) \right] + \sigma \varepsilon_m F_{m,Sp} A_{s_m} T_m^4 + \alpha_m s A_m \cos\theta$$

$$m = 1, 2, \ldots, N; \qquad i = 1, 2, 3 \tag{2}$$

The second term on the right-hand side in Eq. (2) represents the radiation heat transfer to the space, wherein the space temperature is assumed to be 0 K. Only a fraction of the total energy emitting from this element is participating in the radiative heat transfer with other elements. The third term defines the incident solar heat energy on the surface of an element, which is time dependent. Thermophysical properties are assumed to be temperature independent. The internal heat generation is assumed to be uniform within an element.

These equations can be transformed into a set of first-order ordinary differential equations using lumped parameter representation,[11] where each element is subdivided into number of subelements each having a definite volume, but for computational purposes each subelement is identified with a point called a node. The mass of an element is taken to be concentrated at the node. These subelements will be renamed nodal elements. A nodal temperature represents the temperature of the entire nodal element, which is assumed to vary only with time and does not vary with the position within the element. The node may be placed inside or on the surface of the nodal element, depending on the nature of heat transfer taking place between a specific subelement and its neighboring elements. For example, the nodes on the surfaces of the element can have conduction coupling with the adjacent nodes situated inside and radiative coupling with the nodes situated on the surfaces of other elements including space. Some of the external nodes are also exposed to solar radiation. In what follows, we shall consider only nodes. With this background, the second-order temperature derivative with respect to x_1 at ith node can be written as

$$k_{x_1} \frac{\partial^2 T_m}{\partial x_1^2} = \left(\frac{k_{x_1}}{\Delta x_1^2} \right) [T_{i+1}(x_1 + \Delta x_1, x_2, x_3, t) - 2T_i(x_1, x_2, x_3, t) + T_{i-1}(x_1 - \Delta x_1, x_2, x_3, t)] \tag{3}$$

where $i+1$ and $i-1$ are the neighboring nodes that have conduction coupling with the ith node. If there is no neighboring node with conduction coupling in the x_1 direction with the ith node, then the ith node will be shifted to the surface, and instead of conduction, radiation coupling will be considered with the neighboring node, which could also include solar radiation depending on the position of the node. If the ith node does not have conduction coupling with the $(i+1)$th [or $(i-1)$th] node, then the ith node will be shifted to the surface of the subelement on the side of $(i+1)$ [or $(i-1)$ th] node. This does not mean that conduction coupling that was actually there is not accounted for. This is done by generating an extra node for the subelement by subdividing it further in a suitable way. The temperature derivatives with respect to x_2 and x_3 at the ith node can be obtained in a similar way if the conduction coupling in these directions is taking place. For energy balance at the ith node, both conduction and radiation coupling are considered. If the energy balance equation at each node is done in this way, then it is not difficult to obtain the following equation, which incorporates conduction, radiation, solar heat flux, and heat generation terms:

$$m_i c_{p_i} \frac{\mathrm{d}T_i}{\mathrm{d}t} = \sum_{j=1}^{N} \frac{k_{x_j} A_{c_j}}{l_{i,j}} (T_i - T_j) + \sigma \sum_{j=1}^{N} \varepsilon_i F_{i,j} A_{s_i} \left(T_i^4 - T_j^4 \right) + g_i + \alpha_i A_i s \cos\theta, \qquad i = 1, 2, 3, \ldots, N \tag{4}$$

Note in the preceding equation that j can take a maximum of six values out of the N values of i. These six values can be determined only after the discretization of the actual structure.

Sensitivity Function

A conventional definition of a sensitivity function is used. If T_i is the temperature of the ith node and β is some parameter associated with the system, the sensitivity function S_i for a temperature of the ith node is defined by

$$S_i = \frac{\partial T_i}{\partial \beta} \tag{5}$$

For example, if Eq. (4) is differentiated with respect to thermal conductivity k_{x_j}, using the relation in Eq. (5) we get

$$m_i c_{p_i} \frac{\mathrm{d}S_i}{\mathrm{d}t} = \sum_{j=1}^{N} \frac{A_{c_j}}{l_{i,j}} (T_i - T_j) + \sum_{j=1}^{N} \frac{k_{x_j} A_{c_j}}{l_{i,j}} (S_i - S_j) + \sigma \sum_{j=1}^{N} \varepsilon_i F_{i,j} A_{s_i} \left(4T_i^3 S_i - 4T_j^3 S_j \right), \quad i = 1, 2, 3, \ldots, N \tag{6}$$

This forms a system of differential equations defining the sensitivities of all of the nodes with respect to the thermal conductivity k_{x_j}. The system of sensitivity equations with respect to other governing parameters can be generated by differentiating the Eq. (4) separately for each parameter associated with the system.

Semirelative Sensitivity Function

The semirelative sensitivity function[12] S_{r_i} for the ith node is defined as

$$S_{r_i} = \frac{\partial T_i}{\partial \ln \beta} = \frac{\partial T_i}{\partial \beta} \beta = S_i \beta, \qquad i = 1, 2, \ldots, N \tag{7}$$

The semirelative sensitivity function has the dimension of temperature, and it can be used to compare the sensitivities of the ith node with respect to different parameters.

Numerical Computations of Temperatures and Sensitivities

Quasisteady State

To integrate Eqs. (4) and (6), initial conditions are required, which are not known a priori. Therefore, the numerical integration is started with some initial values. For example, the initial values may be taken as zero, and the integration is done for a period of 24 h. The initial values for the second period of 24 h are then taken as the end values of the previous period. The computations are carried out for the successive periods until the absolute differences of the temperatures and sensitivities evaluated at the same time in the nth and $n+1$th period is within some tolerance limit. If the tolerance limit is attained, then the temperatures and sensitivities in the nth period are called quasisteady-state temperatures and sensitivities, respectively. Equations (4) and (6) are to be integrated until the quasisteady state is attained.

Numerical Methods Used

Equation (4) represents a system of nonlinear coupled equations. Once it is solved for quasisteady-state temperatures, Eq. (6) can be solved, which, although it is not nonlinear, is coupled. The systems of Eqs. (4) and (6) have been solved by two different methods. In the first method, a linearization technique is used in conjunction with the Gauss elimination method and an iterative procedure. It is effectively an implicit method. In the second method, the Runge–Kutta–Fehlberg (RKF) method has been used, which is discussed later. The linearization of Eq. (4) can be done as follows.

First Integration Method

The fourth-order term $(T_i^n)^4$ occurring on the right-hand side of Eq. (4) at the nth time step can be written as

$$\begin{aligned}\left(T_i^n\right)^4 &\simeq \left(T_i^{n,r}\right)^4 = \left(T_i^{n,r}\right)^4 - \left(T_e^n\right)^4 + \left(T_e^n\right)^4 \\ &= \left(T_i^{n,r} - T_e^n\right)\left(T_i^{n,r} + T_e^n\right)\left\{\left(T_i^{n,r}\right)^2 + \left(T_e^n\right)^2\right\} + \left(T_e^n\right)^4 \\ &= \left(T_i^{n,r} - T_e^n\right)\left(T_i^{n,r-1} + T_e^n\right)\left\{\left(T_i^{n,r-1}\right)^2 + \left(T_e^n\right)^2\right\} + \left(T_e^n\right)^4 \\ &= D_1 T_i^{n,r} + D_2, \qquad r = 1, 2, 3 \end{aligned} \tag{8}$$

The quantities D_1 and D_2 can be easily written and are given in Eqs. (10) and (11). For $r = 1$, T_e^n can be taken as T_i^{n-1}, and for $r = 2, 3, 4, \ldots,$ T_e^n is replaced by $T_i^{n,r-1}$. In the differential equation for T_i, the term T_j^4, $j \neq i$, is also occurring. The linearization of the term T_j^4 can also be done in the manner just described. The discretized form of Eq. (4) for the rth iteration at the nth time step is

$$\begin{aligned} T_i^{n,r} = T_i^{n-1} + \Bigg[&\sum_{j=1}^{N} \frac{kA_{c_j}}{l_{i,j}}\left(T_i^{n,r} - T_j^{n,r}\right) \\ &+ \sigma \sum_{j=1}^{N} \varepsilon_i F_{i,j} A_{s_i}\left(D_1 T_i^{n,r} - D_2 - E_1 T_j^{n,r} - E_2\right) + g_i \\ &+ \alpha_i A_i s \cos\theta \Bigg] \frac{\delta t}{m_i c_{p_i}}, \qquad i = 1, 2, \ldots, N \end{aligned} \tag{9}$$

where

$$D_1 = \left(T_i^{n,r-1} + T_e^n\right)\left\{\left(T_i^{n,r-1}\right)^2 + \left(T_e^n\right)^2\right\} \tag{10}$$

$$D_2 = -T_e^n\left[\left(T_i^{n,r-1} + T_e^n\right)\left\{\left(T_i^{n,r-1}\right)^2 + \left(T_e^n\right)^2\right\}\right] + \left(T_e^n\right)^4 \tag{11}$$

The quantities E_1 and E_2 can be easily written if the subscript i is replaced by subscript j. If the linearization is done in this way, then a system of linear algebraic equations is obtained, which can be solved by the Gauss elimination method. The temperatures were improved by successive iterations. At each iteration, the Gauss elimination method was used. It may be noted that the coefficient matrix so obtained in the linearized system is diagonally dominant and the method is meaningful only if the successive iterations for the temperatures converge. The successive iterations were found to be converging quickly. The iterations for the temperature at the nth time step were stopped if

$$\left|T_i^{n,r-1} - T_i^{n,r}\right| < 0.005 \qquad \text{for some} \quad r, \qquad i = 1, 2, \ldots, N$$

and later, the computations for the T_i^{n+1} were started. Following the procedure discussed earlier, the quasisteady-state temperatures can be determined. These quasisteady-state temperatures are then used to determine the sensitivity functions. The determination of sensitivity function is not very difficult, as linearization is not required. However, a linear system of equations is once again to be solved, which was done by using the Gauss elimination method.

Second Integration Method

The second integration method used was the RKF method. The algorithm given by Burden et al.[13] was programmed for executing the RKF method to obtain quasisteady-state temperatures and sensitivities. The advantage of this method is that the fourth-order and fifth-order methods can be compared and the time steps are adjusted accordingly. The temperatures and sensitivities obtained from these two methods compare well. The time step used in Gauss elimination method was 100 s, and 72 nodes were considered for both of the integration methods.

Results and Discussion

The configuration of the system of batteries studied in this analysis is described next.

Battery Configuration

Two Ni-Cd batteries are mounted on the extended honeycomb panel of the south panel of the spacecraft, as shown in Fig. 1. Batteries need to be maintained within the temperature range of 0–25°C. The thermal design for the batteries includes a multilayer insulation (MLI) blanket cover, and an optical solar reflector (OSR) is provided on the honeycomb panel to radiate the heat out from the batteries. The optical property values along with the thermophysical properties of the material used are shown in Table 1. The internal details are

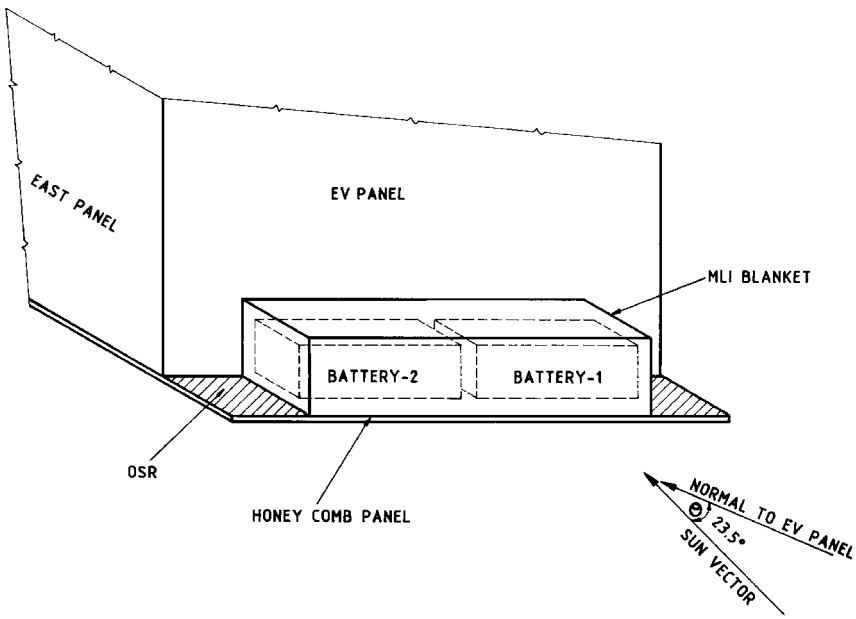

Fig. 1 Schematic of the battery location.

Table 1 Thermophysical and optical properties of various elements

Elements	Solar absorptance, αs	Infrared emittance, ε	Thermal conductance, W/cm^2 K
OSR	0.08 (BOL) 0.21 (EOL)	0.78	
MLI (outer layer)	0.34 (BOL) 0.45 (EOL)	0.67	0.000007[a]
MLI (inner layer)		0.05	
Aluminum honeycomb panel			0.003175[a]
Contact conductance			0.03

[a]Conductance along the thickness.

Table 2 Comparison of RKF method and linearization technique

Method	Function evaluation	Values	CPU time, s
RKF method	Temperature	17.63	700.16
	Semirelative sensitivity[a]	−1.50	1573.52
Linearization technique	Temperature	17.29	324.21
	Semirelative sensitivity[a]	−1.48	285.62

[a]Sensitivities correspond to conductance of the honeycomb panel.

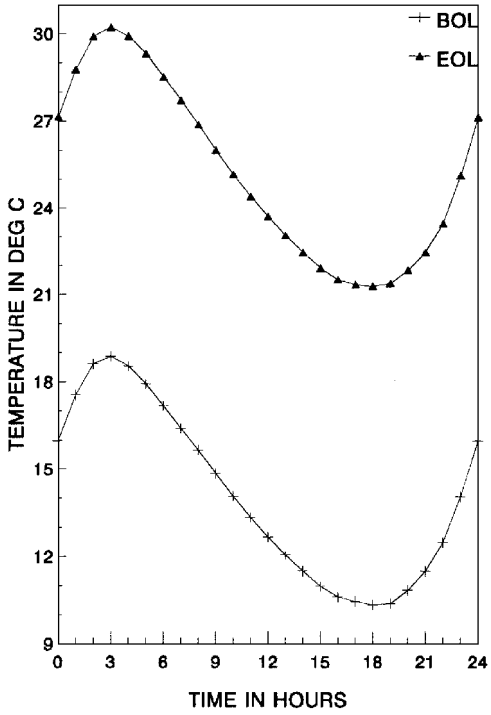

Fig. 2 Variation of temperature of the battery during winter solstice.

not considered here as it is intended to study the sensitivities of battery temperature by considering the interaction of the battery only with its surroundings. The temperature sensitivities of the battery with respect to governing parameters are studied for winter solstice case, and the incident solar heat flux shall be as shown in Fig. 1. A sensitivity study is conducted for two different temperature levels (see Fig. 2), namely, the temperature at the BOL and at EOL of the spacecraft mission, indicating the influence of the degradation of the optical properties.

Comparison of Numerical Methods Used

The temperatures and sensitivities are evaluated using both the described methods. Table 2 compiles the temperatures and its sensitivities to conductance of the honeycomb panel as obtained from linearization technique and RKF method. It appears that the RKF method is computationally more expensive than the linearization method as far as the evaluation of both temperatures and sensitivity

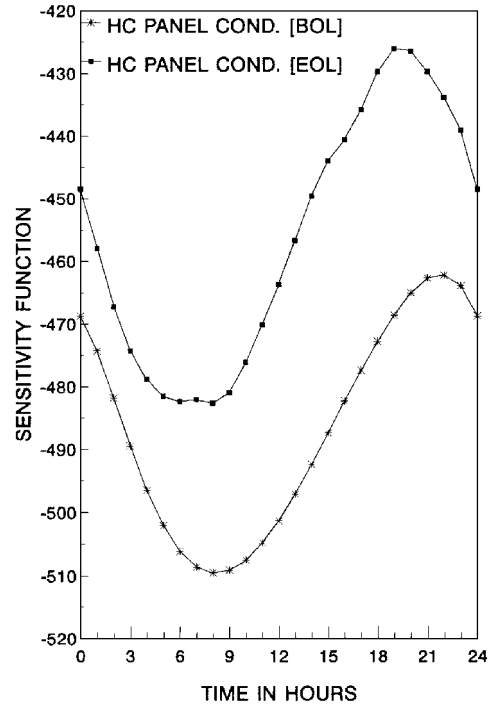

Fig. 3 Temperature sensitivity of the battery with respect to conductance of the honeycomb panel.

functions are concerned. The linearization is required only for the temperature computations. The linearization is not required for the evaluation of the sensitivity function. The choosing of time step in the linearization technique is some what arbitrary, and the accuracy of the results should be checked by reducing the time step. The RKF method, however, has a scheme to adjust time step. Thus, the method of linearization seems to be economical compared to the RKF method.

Comparison of Sensitivities

The sensitivity and semirelative sensitivity study has been conducted for the temperature variation of battery. The sensitivity with various parameters is analysed using temperatures evaluated at BOL and EOL. The results are described in three major groups as conductance, absorptance, and emittance parameters.

Conductance Parameters

Three conductance parameters of the battery system are considered, namely, 1) conductance of the honeycomb panel, 2) conductance of MLI, and 3) contact conductance at the interface between the battery bracket and the spacecraft.

Figure 3 shows the battery temperature sensitivity with respect to the honeycomb panel conductance. In general, the data indicate that this parameter always bears a negative value and thus aids in cooling the battery. It is interesting that the battery temperature attains maximum at around the same time its sensitivity to the conductance also reaches its maximum negative value. As a result, panel conductance can be effectively used to reduce the highest battery temperature. Another observation is that the battery temperature is more sensitive to the honeycomb conductance during BOL than in the EOL. This behavior can be explained in the light of the temperature gradient across the panel. Whenever the battery system receives sun load, the temperature gradient across the panel for EOL is less as compared to that in BOL and thus results in the lower rate of heat transfer across the panel at EOL, minimizing the rate of temperature drop of the battery.

The effect of conductance across the MLI on battery temperature is shown in Fig. 4. Conductance of the MLI also tends to cool the temperature of the battery as is evident from the negative values of sensitivity functions. However, the trend of sensitivities are opposite to the sensitivities corresponding to the honeycomb panel conductance. Smaller difference in sensitivities between BOL and EOL suggests the temperature of the battery

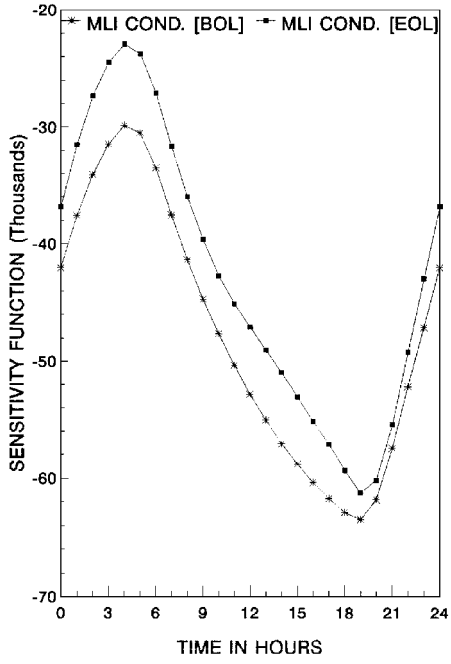

Fig. 4 Temperature sensitivity of the battery with respect to conductance of MLI.

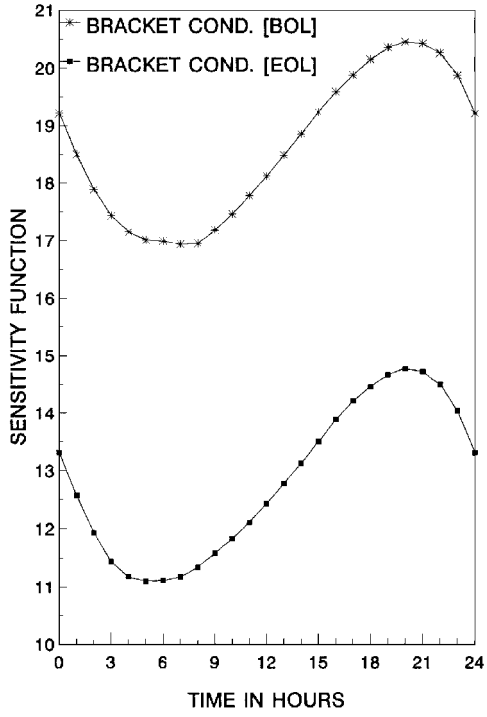

Fig. 5 Temperature sensitivity of the battery with respect to conductance across the battery bracket and honeycomb panel.

will not be affected much due to change in temperature of the MLI.

The temperature sensitivities of the battery for contact conductance at the interface between the spacecraft and the mounting bracket are shown in Fig. 5. Unlike other conductance parameters, this parameter aids in heating the battery as indicated by positive values of the function. Moreover, the rate of temperature rise of the battery becomes more sensitive to this interface conductance during the nonsunlit period of the battery system.

The relative influence of these parameters on the temperature of the battery can be discussed with the help of respective semirelative sensitivity functions. The absolute sensitivity function for conductance of the honeycomb layer is roughly about 1/100th of that of the absolute sensitivity function for conductance of the MLI. This behavior indicates that the MLI conductance is more influential than

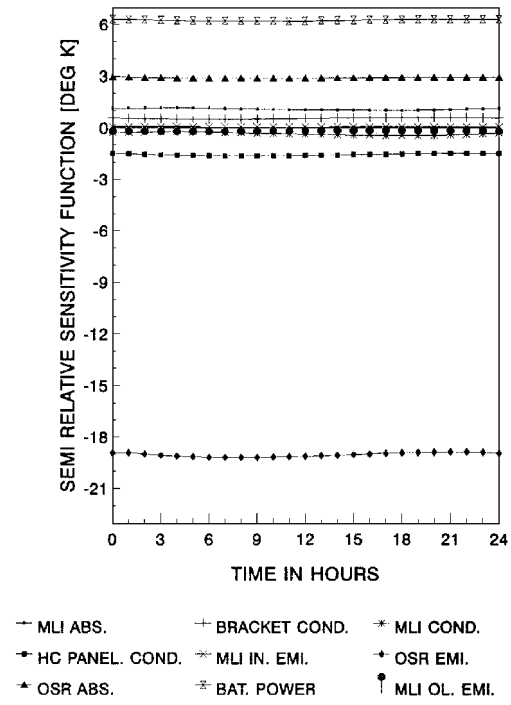

Fig. 6 Semirelative sensitivity function with respect to various parameters for BOL.

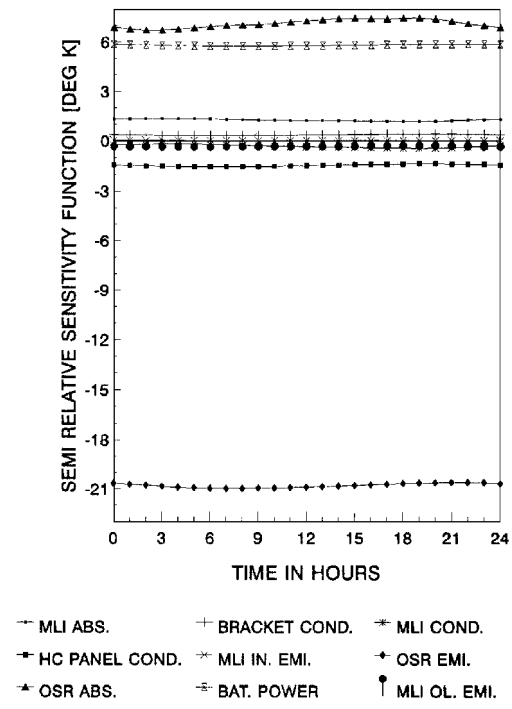

Fig. 7 Semirelative sensitivity function with respect to various parameters for EOL.

the honeycomb conductance. But the semirelative sensitivity functions related to these parameters, as shown in Figs. 6 and 7, exhibit a reverse trend by showing a higher order of magnitude for the honeycomb conductance than the MLI conductance. This explains the dominance of the honeycomb conductance over the MLI conductance in controlling the temperature of the battery.

Absorptance and Power Dissipation Parameters

It is clear from the absolute sensitivity functions shown in Figs. 8–10 that these parameters help in increasing the temperature of the battery. Sensitivities of the battery temperature for all of the absorptance parameters drop from BOL to EOL of the spacecraft mission. Observations pertaining to absorptance of OSR during

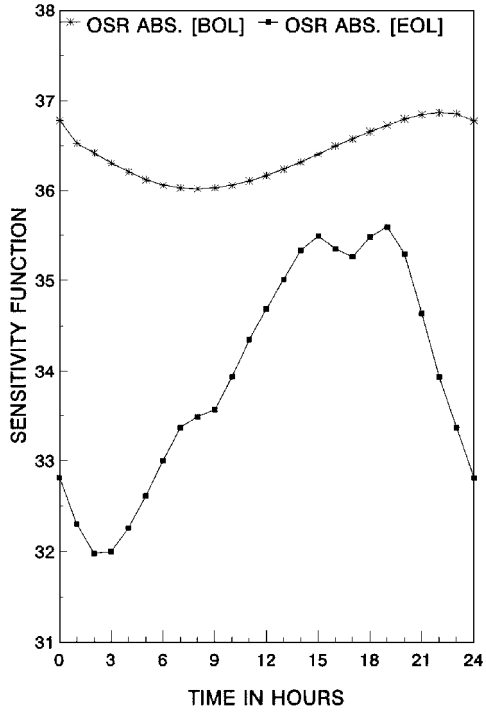

Fig. 8 Temperature sensitivity of the battery with respect to absorptance of OSR.

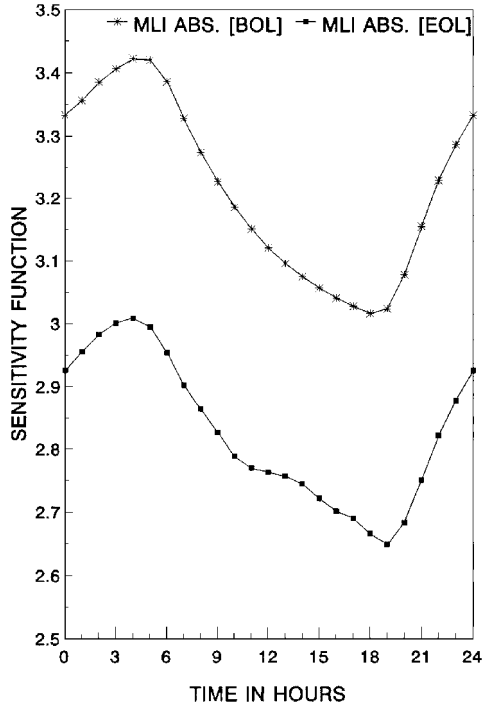

Fig. 9 Temperature sensitivity of the battery with respect to absorptance of MLI.

EOL show that the slope of sensitivity function is higher than during BOL. This is due to degradation of OSR from BOL to EOL resulting in the large difference in heat input to the OSR.

In the winter solstice case, the battery dissipates constant power and these results are shown in Fig. 10. As in the case of contact conductance, the dependence of the temperature of the battery on the power dissipation is realized more in the nonsunlit period.

The significance of relative sensitivity function in the analysis can be illustrated from the study of absorptance of OSR and power dissipation. For example, semirelative sensitivity data corresponding to absorptance of OSR and power dissipation during BOL indicate that the battery is more sensitive to power dissipation in raising its temperature than the absorptance of OSR. However, the EOL data

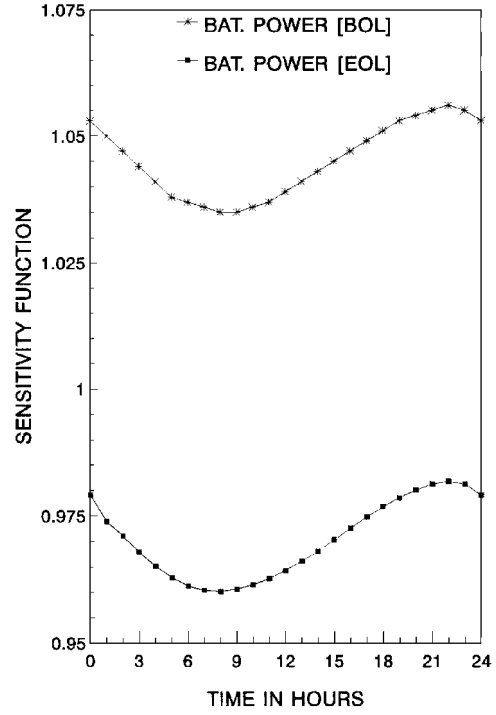

Fig. 10 Temperature sensitivity of the battery with respect to power dissipation of the battery.

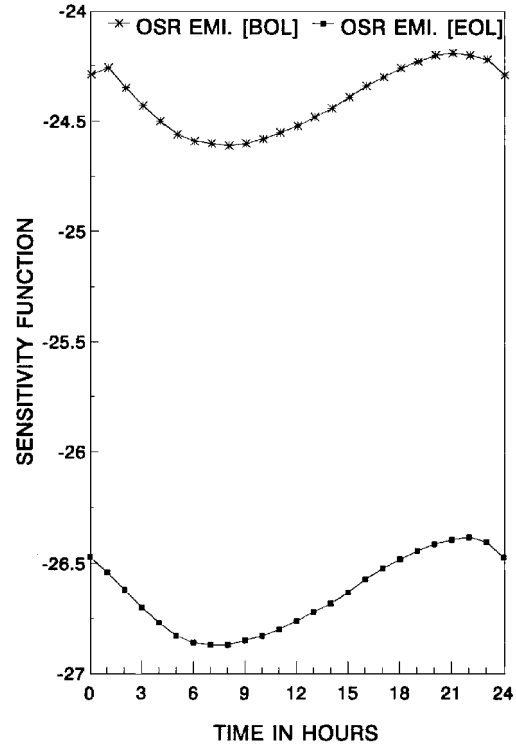

Fig. 11 Temperature sensitivity of the battery with respect to emittance of OSR.

corresponding to these parameters reveal that the higher absorptance of OSR, due to degradation, is sufficient to raise the temperature of the battery in orbit than the power dissipation of the battery in spite of constant and continuous dissipation in the orbit. From the design point of view, therefore, a lower degradation of the surface is preferable for this type of design.

Emittance Parameters

The effect of emittance from various surfaces of the battery configuration, namely, the emittance of OSR and the MLI inner layer and outer layer, on the temperature of the battery is studied with the help of sensitivity functions shown in Figs. 11–13.

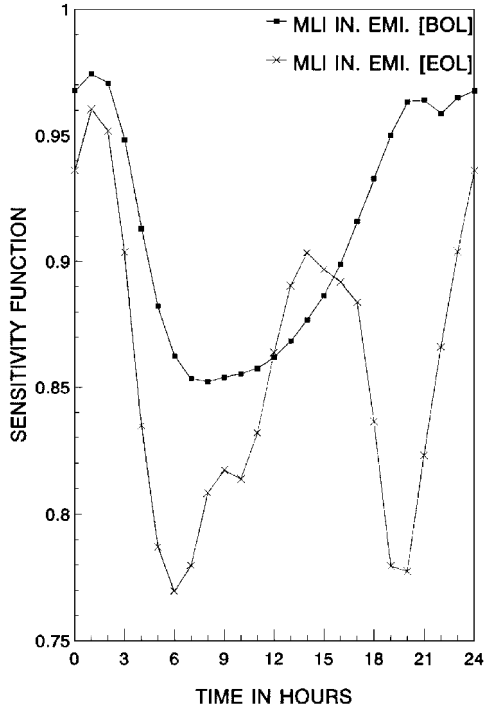

Fig. 12 Temperature sensitivity of the battery with respect to emittance of inner layer MLI.

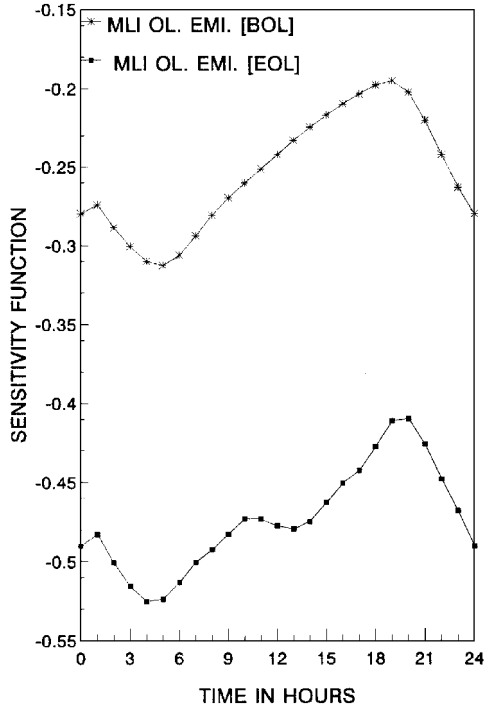

Fig. 13 Temperature sensitivity of the battery with respect to emittance of outer layer MLI.

First, the battery is sensitive to emittance of OSR and the MLI outer layer in reducing its temperature level. The MLI inner layer, however, always supplies heat to the battery. Further, the battery is more sensitive to emittance of OSR at its peak temperatures. This is attributed to the higher temperature of OSR, and subsequently the higher loss of heat from it results in the sensitivity of the battery temperature to be high. Similarly, the lower temperature of OSR is a factor causing the sensitivity function to be lowest when the battery temperature attains its minimum. Similar explanations can be given for the study with respect to emittance of the outer layer MLI also, although its influence on the battery temperature is very negligible.

The difference in sensitivities with respect to emittance of OSR between BOL and EOL is comparatively more than the corresponding difference in sensitivities in case of emittance of the outer layer MLI. This indicates that the battery temperature is less dependent on the change in the MLI outer layer temperature. This phenomenon is analyzed on the basis of availability of the heat-transfer path to the battery from these elements. It is seen that the battery is more thermally coupled with OSR through the honeycomb panel than through the MLI where the heat-transfer path is poor due to the lower conductance across the MLI and lower radiation interaction between the MLI and the battery.

Conclusions

A brief summary of the results of the study is given next.

1) The linearization method adopted here is well suited for the present type of computations.

2) The optical properties of OSR play an important role in controlling the temperature of the battery.

3) In the EOL of the spacecraft, the absorptance of OSR is helpful in adding maximum heat to the battery. However, the power dissipation effect is realized more during the BOL of the spacecraft.

4) The battery temperature was found to be least sensitive for any change in the temperature of the outer layer of the MLI blanket.

5) Increase in absorptance of the external surfaces of the battery configuration results in a decrease in the sensitivity of the battery temperatures.

Acknowledgment

Authors S. Suresha and R. A Katti are grateful to H. Narayana Murthy, Group Director, Thermal Systems Group, Indian Space Research Organisation Satellite Centre, Bangalore, India, for his constant encouragement for this work.

References

[1]Goble, R. G., "Temperature Uncertainties Associated with Spacecraft Thermal Analysis," AIAA Paper 71-430, April 1971.

[2]Haftka, R. T., "Techniques for Thermal Sensitivity Analysis," *International Journal of Numerical Methods in Engineering*, Vol.17, No. 1, 1981, pp. 71–80.

[3]Haftka, R. T., and Malkus, D. S., "Calculation of Sensitivity Derivatives in Thermal Problems by Finite differences," *International Journal of Numerical Methods in Engineering*, Vol. 17, No. 12, 1981, pp. 1811–1821.

[4]Tortorelli, D. A, Haber, R. B., and Lu, S. C.-Y., "Design Sensitivity Analysis for Nonlinear Thermal Systems," *Computer Methods in Applied Mechanics and Engineering*, Vol. 77, Dec. 1989, pp. 61–77.

[5]Lomas, K. J., and Eppel, H., "Sensitivity Analysis Techniques for Building Thermal Simulation Programs," *Energy and Buildings*, Vol. 19, No. 1, 1992, pp. 21–44.

[6]Guru Prasad, K., and Kane, J. H., "Three Dimensional Boundary Element Thermal Shape Sensitivity Analysis," *International Journal of Heat and Mass Transfer*, Vol. 35, No. 6, 1992, pp. 1427–1439.

[7]Wiedemann, M., "Sensitivity Analysis in the Determination of Thermal Parameters," *Hybrid Circuits*, No. 31, May 1993, pp. 29–32.

[8]House, J. M., Arora, J. S., and Smith, T. F., "Comparison of Methods for Design Sensitivity Analysis for Optimal Control of Thermal Systems," *Optimal Control Applications and Methods*, Vol. 14, No. 1, 1993, pp. 17–37.

[9]Johnsee, L., "Modeling and Thermal Management of Advanced Batteries," CONF-880133–3, U.S. Government Printing Office, Washington, DC, May 1988.

[10]"Flight Temperature Predictions of INSAT-2A," INSAT-2A Thermal Design Team, Indian Space Research Organisation Satellite Centre, INTS-TR-MEC-01-90-175(0), Bangalore, India, May 1992.

[11]Collins, R. L., "A Finite Difference Taylor Series Method Applied to Thermal Problems," AIAA Paper 88-2664, June 1988.

[12]Paul, M. F., *Introduction to System Sensitivity Theory*, Academic, London, 1978, pp. 6–18.

[13]Burden, R. L., Faires, J. D., and Reynolds, A. C., *Numerical Analysis*, 3rd printing, Prindle, Weber, and Schmidt, Boston, MA, 1978, pp. 239–258.

I. E. Vas
Associate Editor